

The effect of Cu dopants on electron transfer to O₂ and the connection with acetone photocatalytic oxidations over nano-TiO₂†

Baoshun Liu, ^{*a} Jiangyan Wang,^a Ivan P. Parkin ^b and Xiujian Zhao ^a

Modifying TiO₂ with the Cu element has been shown to be useful for photocatalysis. Although it had been known that Cu species could trap electrons from TiO₂, whether they can affect the kinetics of electron transfer and how this can contribute to photocatalysis still remain unknown. In the current research, Cu–TiO₂ samples were firstly prepared with a hydrothermal reaction and characterized in detail. It was shown that Cu elements were doped in the TiO₂ lattice in +1/0 valence states and have a minor effect on the TiO₂ structure. By means of photoconductances, it is shown that the Cu dopants could catalyze the electron transfer from TiO₂ to O₂ by reducing the apparent activation energy (E_{app}) by about 2 times. The photocatalytic experiments conducted at different temperatures showed that the E_{app} of the acetone photocatalytic oxidations could be decreased by B2 times; this implies that the Cu dopants change the photocatalytic pathway. First-principles computation showed that the surface Cu dopants, along with the compensated oxygen vacancies, can mediate both of the electron and hole transfer. By combining other studies, we proposed that the Cu sites could act as Lewis acid and base pairs that could combine with acetone and O₂ molecules under UV light illumination; this allows electron transfer to O₂ *via* the Cu sites that then react with acetone. As compared to pure TiO₂ surfaces, the different chemical environment of the Cu sites leads to the decrease in the E_{app} of photocatalysis.

1. Introduction

Photocatalysis arises from light generation of the electrons and the holes in the conduction band (CB) and the valence band (VB) of a semiconductor, respectively, as well as their subsequent transfer to reactants, such as O₂ and organics.^{1–3} Under gaseous reaction conditions, the holes transfer to organic molecules, and the electrons mainly transfer to O₂ molecules that are good electron acceptors. For TiO₂ materials, it had been revealed that hole transfer to organics occurs over the ps to ns timescale,⁴ while the electron transfer to O₂ occurs over the ms to ms timescale.^{5–9} It was thought that the photocatalytic activities can be increased if the rate of electron transfer to O₂ can be increased by co-catalysts and dopants.^{10–22}

Our previous study showed that the Au co-catalyst could increase the electron transfer to O₂ by reducing the apparent activation energy (E_{app}).²³ However, it was seen that the increase

in the electron transfer did not lead to an increase in the photocatalytic oxidation of acetone. The E_{app} of photocatalysis also remained unchanged as compared to the undoped TiO₂. On one hand, this result means that the electron transfer to O₂ might not be a limited step of photocatalysis; the electron transfer to O₂ also contributes to the so-called O₂-chemisorption assisted recombination.^{23–25} On the other hand, it was also suggested that

the change in the electron transfer could not naturally mean a change in the photocatalytic pathway, as we expected. This finding raises a problem: what conditions are needed if the change in the electron transfer pathways could change photocatalytic pathways.

The incorporation of Cu into TiO₂ has dual advantages for an antibacterial agent with potential to reduce the recombination of charge carriers.^{26,27} The Cu chemical states can be changed by light illumination.^{28,29} Modifications of TiO₂ materials with Cu have been reported to be useful in photocatalysis. Although it had been revealed that the Cu over TiO₂ surfaces

can act as the site for trapping the electrons in a fast rate over the ps and ns timescale,^{30–33} the fast trapping does not mean a fast transfer to O₂. The current research considers the role of the Cu dopants in catalyzing the electron transfer from TiO₂ to O₂ and whether the photocatalytic pathway could be changed.

Cu doped TiO₂ nanomaterials were prepared with simple hydrothermal reactions. By means of photoconductance decays,

^a State Key Laboratory of Silicate Materials for Architectures, Wuhan University of Technology, Wuhan City, Hubei province 430070, P. R. China.

E-mail: liubaoshun@126.com

^b Department of Chemistry, Materials Chemistry Centre, University College London, 20 Gordon Street, London WC1H 0AJ, UK

we showed that the Cu dopants can catalyze the electron transfer from nano-TiO₂ to O₂ as the E_{app} of the electron transfer was decreased. It was also shown that the E_{app} of photocatalytic acetone oxidations was decreased to some extent; this might imply that the photocatalysis could occur over the Cu sites and so the photocatalytic pathway could be changed. First-principles calculation showed that the Cu dopants, along with the compensated oxygen vacancies, are capable of mediating both the electron and hole transfer. Based on those findings and combined other literature, it was proposed that the Cu sites could act as the spots on which the Lewis acid and Lewis base sites co-exist under light illumination; this allows the electron transfer to O₂ *via* the Cu sites, which could then react with the adjacent hole trapped acetone. The E_{app} of the photocatalysis was decreased due to the different chemical properties as compared to pure TiO₂ surfaces. Thus, whether the dopants could be sites that can simultaneously assist electron and hole transfer, and allow subsequent reactions between electron and hole trapped species should be a prerequisite that the change in electron transfer to O₂ could change the photocatalytic pathway. This finding gains some deep insights into the mechanism of photocatalysis, and could be a guiding set of principles for designing highly active materials.

2. Experimental

2.1. Sample preparation

TiO₂ anatase nanoparticles were prepared with an agitation-assisted hydrothermal method. HF was also added to increase the ratio of exposed {001} facets to increase the photocatalytic activity of nano-TiO₂. Firstly, 3.3 mL of HF aqueous solution (40 vol. %) and 12 mL of ultrapure water were mixed in a Teflon-sealed steel reactor. Then, 15 mL of tetrabutyl titanate (TBOT) was dropped in the reactor with continuous stirring for 10 min, which was then placed in an oil bath for hydrothermal reactions at 180 °C for 12 h under simultaneous stirring (600 r min⁻¹). Then the reactor was cooled down to room temperature. The precipitate was transferred to a beaker and washed three times with deionized water and absolute ethanol, respectively. The sample was then dried and ground to get the final TiO₂ powders. Synthesis of the Cu doped TiO₂ sample (Cu-TiO₂) is basically the same as the preparation of TiO₂ except that 0.2 g of CuCl₂•H₂O were added as reactants.

2.2. Characterization

Surface images of the TiO₂ and Cu-TiO₂ samples were observed with a field emission scanning electron microscope (FE-SEM; type: S-4800, Hitachi, Tokyo, Japan) and a field emission transmission electron microscope (TEM; type: JEM2100F, JEOL, Tokyo, Japan). X-Ray diffraction (XRD) patterns were collected with a grazing incidence X-ray diffraction meter (XRD; Empyrean, PANalytical, Almelo, Netherland) with the Cu K α radiation being used as the X-ray source. The surface chemical compositions of the pure TiO₂ and Cu-TiO₂ samples were checked with an X-ray photoelectron spectrometer (XPS; type: VG Multilab 2000, Thermo

Scientific, Waltham, America), with an X-ray source working with the Al K α radiation using the binding energy (284.6 eV) of C1s electrons as the energy reference. UV-vis diffused spectra of the samples were recorded by using a UV-Vis photo spectrometer within the wavelength range from 200 nm to 800 nm (type: UV-3600, Shimadzu, Tokyo, Japan).

2.3. Catalytic property measurement

Photocatalytic experiments were conducted in a self-designed quartz glass closed-circulation cylindrical batch reactor. A Pt100 resistance thermometer detector (RTD) was used to monitor the reaction temperatures. The reactor was heated to a set temperature between 20 °C and 90 °C using a heating plate. A xenon lamp equipped with a 365 nm band-pass optical filter was used as the light source for the photocatalytic reactions. 365 nm light ensures that TiO₂ was excited, so the role of the Cu dopants in modulating charge carrier transfer could be discussed. The light intensity was kept at 0.20 mW cm⁻² for all experiments, which was monitored with a Si diode photodetector (Newport 843-R).

0.1 g of the undoped TiO₂ and Cu-TiO₂ samples were dispersed ultrasonically with pure water in 50 mm glass containers. After heating to remove water, a thin coating of the sample formed on the container bottom was used for acetone photocatalysis. The samples were firstly pre-treated by UV light illumination for 24 h to remove carbonate contaminants before starting photocatalytic reactions. Clean air was flowed through the reactor for 15 min until the residual CO₂ concentration was lower than 20 ppm. Acetone was used for photocatalytic oxidations. The reactor containing the samples was firstly kept in the dark for 45 min at the set temperature. Subsequently, 2 mL of liquid acetone was injected into the reactor, which was kept in the dark for another 45 min to allow an adsorption-desorption equilibrium. Then, the 365 nm UV light was switched on to illuminate the samples for 140 min. The concentration of acetone and CO₂ was monitored in line with a gas chromatograph (Shimadzu 2016) equipped with a methane convertor. The initial rates of CO₂ generation under light illumination were used to evaluate the photocatalytic activity.

2.4. Vacuum photoconductance measurement

Vacuum conductances were measured in a self-designed setup that contains an electrical conductance measurement chamber, a vacuum pump system, an atmospheric control system, a temperature-control system, and a light source (Fig. S1, ESI†). An INSTEC chamber containing a temperature-programmed sample platform and four probes for electric conductance measurement was the main part. The top cover of the chamber (not shown here) contained a piece of quartz glass for normal light illumination. The temperatures were under accurate control *via* an electric heating and a liquid N₂ cooling system. The chamber was evacuated to below 1 m Torr using a mechanical pump and a molecular pump. The effect of UV light illumination on the vacuum conductance was measured at different temperatures and constant O₂ partial pressure (1.0 Pa). The 365 monochromic light generated from a xenon lamp equipped with a band-pass optical filter was used as the light source.

A thin coating was prepared on a quartz glass substrate by doctor-blading the aqueous dispersion of the sample. After it had dried, two gold thin film electrodes were deposited on the coating and a 0.2 mm TiO₂ strip was left for conductance measurements. The electric conductance was recorded with a two-probe mode with 1.0 V voltage drop between the two Au electrodes.

2.5. First principles calculation

Periodic three-dimensional first principles calculations were carried out using the open-sourced Quantum-ESPRESSO software package.³⁴ In the calculations, the energy was computed using the generalized gradient approximation (GGA) of DFT proposed by Perdew, Burke, and Ernzerhof (PBE) and the

ultrasoft pseudopotentials were used to describe the exchange correlation effects and electron ion interactions. The kinetic

energy cutoffs of 24 and 288 Ry for the smooth part of electronic wave functions and augmented electron density were used. Forces on the ions were calculated through the Hellmann–Feynman theorem, including the Harris-Foulkes correction. The geometry optimization calculation was performed before electronic structure calculation using the conjugated gradient algorithm. Iterative position relaxation of all atoms was stopped until the forces on atoms were less than 0.01 eV Å⁻¹. Monkhorst–Pack (M–P) *k*-space sampling was adopted for SCF calculations. The convergence threshold for the self-consistent energy calculation was set to 10⁻⁸ Ry.

Copper doped anatase was calculated using the supercell methodology. The bulk doped anatase TiO₂ was modeled with a 48-atom (2 × 2 × 1) supercell, with a Ti atom being replaced with a Cu atom. The slab model was used to construct an anatase (101) surface. The surface was represented by three-layer slabs made of 2 × 3-unit cells; this is enough to assess the Cu dopant. A vacuum space (20 Å) of sufficient separation was imposed to ensure no interaction with the lowest layer of the upper slabs. A 5-fold Ti atom was replaced with a Cu atom to model the TiO₂ surface doped with the Cu dopant. In addition, a 2-fold O atom adjacent to the Cu atom was also removed to model the surface Cu dopant along with an O vacancy. The density of states (DOS) of Ti3d, Cu3d, and O2p were obtained and plotted with respect to the energy to see the effect of the Cu dopant on the electronic structure of anatase TiO₂.

3. Results and discussion

3.1. Physical property characterization

The XRD patterns of the pure and Cu–TiO₂ sample were well indexed to the anatase phase of TiO₂ (JCPDF 99-0008) (Fig. S2, ESI†).³⁵ No diffraction peaks of metal Cu or Cu oxides were observed. The TiO₂ grain sizes estimated from the Scherrer equation are 15.3 nm and 12 nm for the pure TiO₂ and Cu–TiO₂, respectively; this shows that the Cu doping leads to a slight decrease in crystallinity. Raman spectroscopy was also employed to see the effect of Cu doping on the crystalline structure (Fig. S3, ESI†). All of the Raman scattering peaks

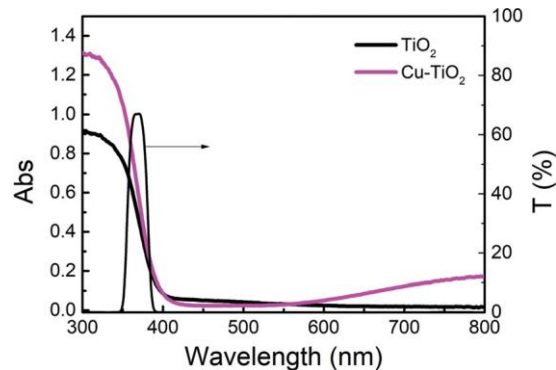


Fig. 1 UV-Vis diffusion absorption spectra of the pure and Cu–TiO₂ samples and the transmittance spectra of the 365 nm band-pass optical filter.

correspond to the vibration modes of anatase TiO₂,³⁵ in agreement with the XRD analysis. The Raman characteristic peaks of Cu₂O and CuO do not appear,^{36,37} showing no detectable Cu oxides in the Cu-doped sample. Magnification of the *E_g* vibration peak shows that the Cu doping has no effect on the peak's position and half-width. The specific surface areas of these samples were 78 m² g⁻¹ and 83 m² g⁻¹, respectively. The Cu content in Cu–TiO₂ was about 0.5 at%, as determined from ICP-OES.

UV-visible diffuse reflectance spectra of the undoped TiO₂ and Cu–TiO₂ samples are shown in Fig. 1. Cu doping has no effect on the absorption edge of TiO₂. The Cu–TiO₂ sample presents a visible and near-IR light absorption above 550 nm.^{38,39} The UV-Vis result implies that the Cu atoms should be doped in TiO₂, although they have no effect on the TiO₂ crystalline structure. The transmittance spectrum of the 365 nm band-pass optical filter is also shown, which was used to generate the UV light for photocatalytic and photoconductance measurements by exciting the VB to CB electronic transition.

The O1s, Ti2p, and F1s core-level XPS spectra of TiO₂ and Cu–TiO₂ are shown in Fig. S4–S6 (ESI†), respectively. The surface oxygen species include lattice oxygens and surface-capped hydroxyl groups.⁴⁰ The relative contents of the hydroxyl groups are 15.6 at% and 16.3 at% for the pure and Cu–TiO₂ samples, respectively. As the normalized Ti2p spectra are almost the same, the Cu dopants also do not affect Ti chemical states, mainly existing in 4⁺^{41,42} The atomic ratios of F on the surfaces of the pure TiO₂ and Cu/TiO₂ are 5.73 at% and 5.43 at%, respectively, showing that the Cu doping also does not affect F content. Fig. 2 shows the Cu2p core-level XPS spectra. The Cu2p_{1/2} and Cu2p_{3/2} peaks are at 951.9 eV and 932.1 eV, respectively, showing the presence of Cu in +1 or 0 valence states.^{43,44} The Cu2p_{3/2} can be well fitted with a single peak. The lack of the Cu(II) shake-up satellite peak that is normally found around 945 eV indicates the absence of Cu(II) on this surface. Alotaibi *et al.* also found that the low-level doping in TiO₂ mainly exists in the Cu(I)/Cu(0) state.⁴⁵

FE-SEM images of the undoped TiO₂ (Fig. S7, ESI†) and Cu–TiO₂ (Fig. S8, ESI†) show that they are composed of uniform aggregated nanoparticles. TEM images of the undoped TiO₂ (Fig. 3A) and

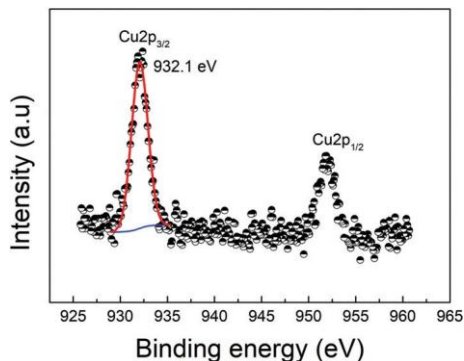


Fig. 2 Cu2p core-level XPS spectrum of the 0.2 Cu-TiO₂ sample.

Cu-TiO₂ (Fig. 3B) show that the nanoparticle sizes of the two samples are almost the same, in accordance with the XRD analysis. Some nanoparticles exist in the form of truncated octahedrons and nanosheets because fluoride acid limits the growth along the [001] direction. Suitable exposition of {101} facets is beneficial for photocatalytic properties.^{46,47} Clear lattice fringes corresponding to the (101) planes of anatase TiO₂ can be seen in the high-resolution (HR-) TEM images (Fig. 3C and D). Cu_xO nanoparticles or nanoclusters are not seen, so the above analysis concluded that the Cu ions were doped in TiO₂ lattices. This is also in good agreement with the study that reported the

formation of the Cu-O-Cu state at a low doping level.⁴⁸

3.2. Photoconductance analysis

The kinetics of the electron transfer from the TiO₂ samples to O₂ was studied by electric photoconductances at different temperatures (Fig. S9 and S10, ESI†) under constant oxygen

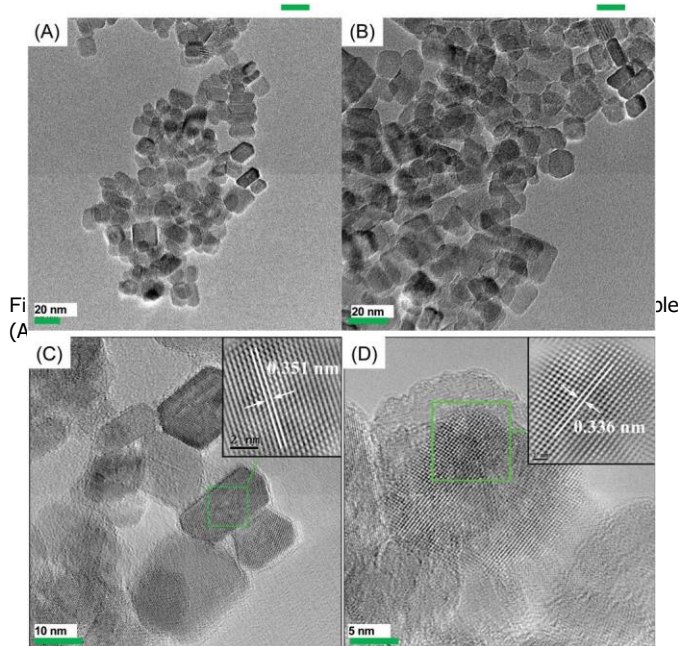


Fig. 3 TEM images of (A) TiO₂ and (B) Cu-TiO₂ samples. (C) HR-TEM image of TiO₂ and (D) HR-TEM image of Cu-TiO₂ samples.

partial pressure (1.0 Pa) and at constant light intensity (20 mW cm⁻²). The conductances show a slow increase after the turning-on of light illumination for both the pure and Cu-TiO₂ samples. This phenomenon was also observed in other studies when the oxygen partial pressure was low.^{49,50} The slow light-desorption of the chemisorbed O₂ might contribute to this slow increase of the photoconductances.⁵¹ The long-time persistent relaxation of the photoconductances after the turning-off of the light illumination is ascribed to the low O₂-chemisorption assisted recombination in the absence of organics; this is also in accordance with other reports conducted under similar experimental conditions.^{52,53} The highest photoconductances of the pure TiO₂ and Cu-TiO₂ decrease and increase with the increase of temperatures, respectively (Fig. S11, ESI†). The electron transfer to O₂ is the only way for the electron extraction from the TiO₂ samples; this indicates that the temperature has a larger effect on the electron transfer kinetics for the pure TiO₂ as compared to Cu-TiO₂.

Hall effect measurement has revealed that the electron mobility of nano-TiO₂ materials is almost independent of light illumination,⁵⁴ so it can be considered that the density of electrons in TiO₂ is proportional to the photoconductances. Taking the single electron transfer into consideration (e + O₂ → O₂⁻), the kinetics of the electron-to-O₂ transfer is slimly described with a quasi-first order reaction.

$$\ln\left(\frac{n(t)}{n(0)}\right) = \ln\frac{\sigma(t)}{\sigma(0)} = -k_e t \quad (1)$$

where $n(t)$, $s(t)$, $n(t)$ and $s(0)$ denote the transient electron density and photoconductances at time t and 0 just after the termination of light illumination, and k_e is the rate constant of the electron transfer to O₂. The persistent relaxation of the photoconductances is re-plotted according to eqn (1) for the two samples (Fig. S12 and S13, ESI†), respectively. The k_e values were obtained by fitting the lines of Fig. S12 and S13 (ESI†). The Arrhenius plots of the obtained k_e values are shown in Fig. 4. The E_{app} values of the electron transfer to O₂ are 13.5 kJ mol⁻¹ and 4.6 kJ mol⁻¹ for the pure TiO₂ and Cu-TiO₂ samples, respectively. The above result showed that the rate of the electron transfer to O₂ was increased by the Cu dopants over all the studied temperatures. Therefore, the decrease of the E_{app} also confirmed the role of

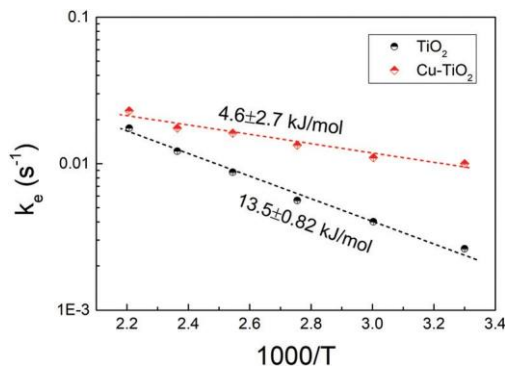


Fig. 4 Arrhenius dependences of the rate constants of electron interfacial transfer to O₂ for TiO₂ and Cu doped TiO₂ samples.

the Cu dopants in acting as a bridge for increasing the electron transfer to O₂.

3.3. Photocatalytic studies

To check whether the Cu dopants have an effect on the E_{app} of the photocatalysis, the acetone photocatalytic oxidations over the undoped TiO₂ and Cu–TiO₂ were conducted at different temperatures (Fig. S14 and S15, ESI†). The decrease of the initial CO₂ evolutions when the reaction temperature is 80 IC and 90 IC is due to carbonate deposition on the surface.¹ We used the photocatalytic oxidations at 30, 40, 50, and 70 IC to analyze the apparent kinetics. The Arrhenius plots of the CO₂ evolution rates are shown in Fig. 5. The E_{app} of the photocatalytic reactions over the pure TiO₂ and Cu–TiO₂ samples were estimated to be 8.3 kJ mol⁻¹ and 3.0 kJ mol⁻¹, respectively. The low E_{app} of the CO₂ evolution is also in accordance with our previous studies.^{1,2} Despite the small E_{app} , the result still reveals the function of the Cu dopants in changing the photocatalytic pathway as the E_{app} is reduced by 2 times; this makes the photocatalysis over Cu–TiO₂ almost independent of temperature, as compared to the undoped sample. This result showed that the acetone photocatalytic oxidations could occur over the Cu dopant sites, and the Cu dopants provide the active sites for the photocatalysis to occur. Different from other studies that observed an increase of photocatalytic activity after Cu doping,⁴⁵ our result shows that the photocatalytic activity was decreased at temperatures higher than 30 IC. The decrease in the E_{app} does not lead to an increase in photocatalytic activity, indicating that the Cu dopants may reduce the number of electrons that can participate in the photocatalysis. In addition to the electron transfer to O₂, the Cu dopants in the TiO₂ lattice may also increase the recombination. It is also seen that the E_{app} of the photocatalysis is different from that of the electron transfer to O₂; this means that the electron transfer to O₂ could not be a limited step for the whole photocatalysis over both the undoped and Cu-doped TiO₂ samples. In addition to the hole transfer and electron transfer, other subsequent processes, including the reaction between electron trapped O₂ and hole trapped organics, the desorption of products, could be

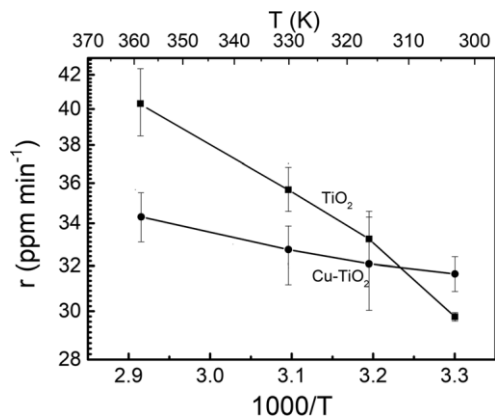


Fig. 5 Arrhenius plots of the acetone photocatalytic oxidations over the undoped and Cu doped TiO₂ samples.

the limited step of photocatalysis. Here, the lower E_{app} of the photocatalysis does not mean a faster rate as compared to the electron transfer because the reaction rates are also dependent on other factors, such as reactor concentrations, in addition to the thermal barrier. Therefore, our results showed that the electron transfer to O₂ is faster than the photocatalytic reactions. Based on our previous study,^{1,23} we thought that the Cu dopants also increase the O₂-chemisorption assisted recombination; this might be one reason for the photocatalytic activity above 30 IC to become lower as compared to the undoped sample.

3.4. First-principles computation

First-principles calculations were performed to show the effect of Cu dopants on the electronic structure of TiO₂, so as to connect the charge carrier transfer with the photocatalytic oxidations. The total DOS of the undoped bulk TiO₂ (Fig. S16, ESI†) shows that the VB and CB are mainly composed of O2p-derived VB states and the Ti3d-derived CB states, separated by a forbidden band. A clear intermediate gap state, arising from the empty hybridization between Cu3d and O2p orbitals, appears in the band gap, for the bulk TiO₂ lattice with a Ti atom being replaced with Cu (Fig. S17, ESI†). In this case, the gap states could capture the photoinduced electrons and can then recombine with the holes, so the bulk Cu dopants should act as the recombination centers. The Cu dopants on surfaces are in direct connection with the charge carrier transfer, so we compared the DOS of the following three cases. The total DOS of the pure TiO₂ (101) surface does not show an intermediate gap state (Fig. S18, ESI†). When one 5-fold Ti atom was replaced with a Cu atom, a clear Cu3d–O2p hybridization-derived gap state appears in the band gap; the Fermi level shifts to the VB top (Fig. S19, ESI†). In this case, the gap states should mainly play the role of electron trap and thus affect the electron transfer. In general, the charge compensation effect requires that doping Cu in the TiO₂ lattice is accompanied by the formation of oxygen vacancies. A bridging oxygen adjacent to the surface Cu dopant was removed to model this case. Fig. 6 shows the DOS of Ti3d, Cu3d, and O2p. A similar half-occupied Cu3d–O2p hybridized gap state appears in the gap. This gap state is thus capable of mediating both the electron transfer and hole transfer due to the half-filled feature; this may allow the reaction of O₂⁻ with the hole trapped organics over the Cu dopant region.

3.5. Proposed mechanism

Based on the above results, a possible pathway for the photocatalytic oxidation over the Cu dopant region is proposed in Fig. 7. The availability of the Lewis acid sites is essential for anchoring acetone molecules to TiO₂ surfaces for photocatalytic reactions.⁵⁴ For example, it was seen that acetone molecules were irreversibly adsorbed *via* Z¹-coordination to the Lewis acid sites (uncoordinated Ti sites) on TiO₂ surfaces in the form of ((CH₃)₂CQO – Ti⁴⁺).⁵⁵ The α -hydrogen of acetone ligands can be abstracted, provided that the coordinate sites are strongly acidic, and has a basic site (surface –OH⁻ or O₂⁻). In addition

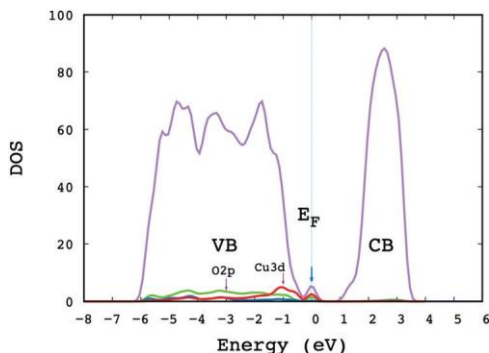


Fig. 6 DOS of the Cu-doped TiO₂ (101) surface along with an additional oxygen vacancy.

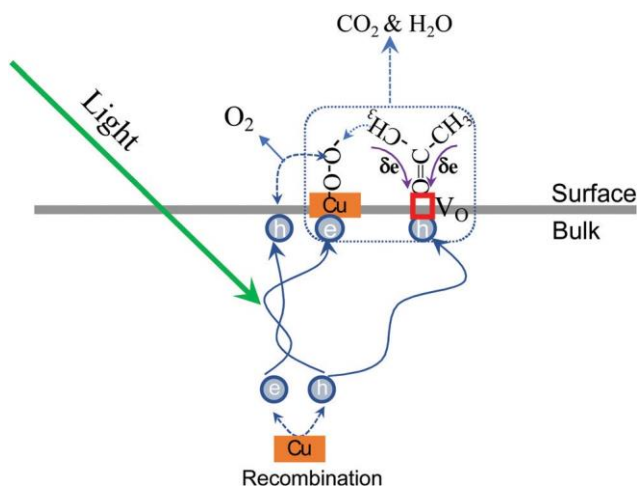


Fig. 7 Diagram of the role of Cu dopants in acetone photocatalytic oxidation through the synergism between hole transfer and electron transfer and charge carrier kinetic processes.

to the uncoordinated cationic Ti ions, oxygen vacancies are also the Lewis acid sites.⁵⁶ The formation of the compensated oxygen vacancies adjacent to the Cu sites on the TiO₂ surface was also confirmed by EPR.⁵⁷ The carbonyl group of the acetone molecules could play the role of a Lewis base site because it has an isolated electron pair and can combine with oxygen vacancies *via* Z¹-coordination. The Cu sites at the TiO₂ surfaces could assist the electron transfer to O₂, as revealed by the photoconductance results; this can lead to chemisorption of O₂ on the Cu sites and might form Cu⁺ O-O⁻ groups. The Cu⁺ O-O⁻ group contains an electron in the anti-bonding orbital of the adsorbed O₂, and thus becomes a strong Lewis base site at the Cu doped region. Therefore, Cu⁺ O-O⁻ can combine with the methyl group of acetone to form Cu⁺ O-O⁻... (CH₃)₂CO - V_o chain at the Cu doped region.

The first-principles calculation showed that the Cu site can also trap holes because of the half-filled state, so the compensated V_o can catalyze the hole transfer to acetone molecules. A more electron cloud at the α -hydrogen of acetone will be pulled toward the carbonyl group and the oxygen vacancy, which makes the

α -hydrogen more acidic. In this case, the α -hydrogen abstraction from acetone to Cu⁺ O-O⁻ becomes possible, and can lead to acetone oxidation under UV light illumination. From this viewpoint, we proposed that the surface Lewis acid (Cu site) and base (V_o) pairs functioning in a concerted fashion allows the reactions of O₂⁻ and the hole trapped acetone at the same Cu doped region. This is also in accordance with Zaki's finding that the coexistence of acid and base sites could catalyze the acetone into mesityl oxide surface species.^{54,58} Thus, the electron transfer from TiO₂ to O₂ through the Cu dopants could contribute to the photocatalytic reactions, in addition to the O₂-sorption assisted recombination. As the E_{app} of the photocatalysis was changed, the different chemical environment of the Cu regions can change the photocatalytic pathway.

The Cu site regions should contribute to the photocatalysis by accelerating the electron transfer to O₂, as shown in Fig. 4. However, Fig. 5 further shows that the photocatalytic activities at temperatures higher than 30 °C become lower than that of undoped TiO₂ although the E_{app} is decreased. This result means that the Cu dopants should also lead to a decrease of the number of charge carriers that could participate in the photocatalysis over the Cu sites. The electrons transferring to O₂ could also undergo O₂-chemisorption assisted recombination parallelly in addition to the photocatalytic reactions.²³ In addition, the Cu dopants located in the bulk mainly play a role in recombination. Therefore, the decrease in the E_{app} of the photocatalysis does not naturally lead to an increase in the photocatalytic activity, because the number of charge carriers that could contribute to the photocatalysis might also decrease. Many works, including our previous works, only studied the effect of dopants on photocatalysis at room temperature (below 30 °C),^{15,16,39,45} and an increase in the photocatalytic activity was observed; this is also in accordance with our current study. We studied the temperature effect and the results lead to more comprehensive understanding of doped TiO₂ photocatalysis.

4. Conclusions

In summary, our results confirmed that Cu dopants can change the pathway of the electron transfer from TiO₂ to O₂; the E_{app} of the electron transfer was decreased by B2 times as compared to that of the undoped sample. It was also seen that the E_{app} of the acetone photocatalytic oxidations was also changed by the Cu dopants. The E_{app} of the photocatalysis was decreased by nearly 3 times, showing a change in the photocatalytic pathway. First-principles calculations showed that the surface Cu dopants, along with compensated oxygen vacancies, could mediate both the electron transfer to O₂ and the hole transfer to organics. Under light illumination, it was proposed that the Cu sites have dual functions of Lewis acid and Lewis base sites; this allows the photocatalytic reactions to occur over the Cu sites. Due to the different chemical environments, the E_{app} of the photocatalysis was decreased. Our results suggested that the increase of the electron transfer could change the photocatalytic pathway if there is a synergistic reaction between the

electrons transferring to O₂ and holes transferring to acetone at the same Cu site.

Conflicts of interest

There are no conflicts to declare.

Acknowledgements

B. Liu acknowledges the National Natural Science Foundation of China (No. 51772230) and National Key Research and Development Program of China (No. 2017YFE0192600). B. Liu also acknowledges the Open Foundation of Key Laboratory for UV-Emitting Materials and Technology of Ministry of Education, Northeast Normal University (Grant No. 135130013) and Key R&D project Hubei Province, China (Grant No. 2020BAB061). We thank Dr Daibing Luo from Analytical@Testing Center of Sichuan University for his help in structural analysis. Professor Parkin thanks the Chinese government for 101 project and Wuhan Technological University for a visiting professorship, and EPSRC M3S CDT project (EP/L015862/1).

References

- 1 B. Liu, H. Wu and I. P. Parkin, New Insights into the Fundamental Principle of Semiconductor Photocatalysis, *ACS Omega*, 2020, 5, 14847–14856.
- 2 B. Liu, H. Wu and I. P. Parkin, Gaseous Photocatalytic Oxidation of Formic Acid over TiO₂: A Comparison between the Charge Carrier Transfer and Light-Assisted Mars–van Krevelen Pathways, *J. Phys. Chem. C*, 2019, 123, 22261–22272.
- 3 A. Stevanovic and J. T. Yates Jr., Electron Hopping through TiO₂ Powder: a Study by Photoluminescence Spectroscopy, *J. Phys. Chem. C*, 2013, 117, 24189–24195.
- 4 T. Yoshihara, R. Katoh, A. Furube, Y. Tamaki, M. Murai, K. Hara, S. Murata, H. Arakawa and M. Tachiya, Identification of Reactive Species in Photoexcited Nanocrystalline TiO₂ films by Wide-wavelength-range (400–2500 nm) Transient Absorption Spectroscopy, *J. Phys. Chem. B*, 2004, 108, 3817–3823.
- 5 B. Liu, X. Zhao, J. Yu, I. P. Parkin, A. Fujishima and K. Nakata, Intrinsic Intermediate Gap States of TiO₂ Materials and Their Roles in Charge Carrier Kinetics, *J. Photochem. Photobiol., C*, 2019, 39, 1–57.
- 6 Y. Tamaki, K. Hara, R. Katoh, M. Tachiya and A. Furube, Femtosecond Visible-to-IR Spectroscopy of TiO₂ Nanocrystalline Films: Elucidation of the Electron Mobility Before Deep Trapping, *J. Phys. Chem. C*, 2009, 113, 11741–11746.
- 7 X. Li, A. N. M. Green, S. A. Haque, A. Mills and J. R. Durrant, Light-driven oxygen scavenging by titania/polymer nanocomposite films, *J. Photochem. Photobiol., A*, 2004, 162, 253–259.
- 8 A. Yamakata, T. Ishibashi and H. Onishi, Water- and Pt/TiO₂: A Oxygen-Induced Decay Kinetics of Photogenerated

- Electrons in TiO₂ and Time-Resolved Infrared Absorption Study, *J. Phys. Chem. B*, 2001, 105, 7258–7262.
- 9 A. M. Peiró, C. Colombo, G. Doyle, J. Nelson, A. Mills and J. R. Durrant, J. R. Photochemical Reduction of Oxygen Adsorbed to Nanocrystalline TiO₂ Films: A Transient Absorption and Oxygen Scavenging Study of Different TiO₂ Preparations, *J. Phys. Chem. B*, 2006, 110, 23255–23263.
- 10 L. Clarizia, R. Andreatti, J. Apuzzo, J. D. Somma and R. Marotta, Efficient Acetaldehyde Production and Recovery upon Selective Cu/TiO₂-Photocatalytic Oxidation of Ethanol in Aqueous Solution, *Chem. Eng. J.*, 2020, 393, 123425.
- 11 C. Burda, Y. Lou, X. Chen, A. C. S. Samia, J. Stout and J. L. Gole, Enhanced Nitrogen Doping in TiO₂ Nanoparticles, *Nano Lett.*, 2003, 3, 1049–1051.
- 12 S. Varnagir, A. Medvids, M. Lelis, D. Milcius and A. Antuzevic, Black Carbon-doped TiO₂ Films: Synthesis, Characterization and Photocatalysis, *J. Photochem. Photobiol., A*, 2019, 382, 111941.
- 13 L. Zhang, B. Han, P. Cheng and Y. H. In-situ, FTIR-DRS Investigation on Shallow Trap State of Cu-doped TiO₂ Photocatalyst, *Catal. Today*, 2020, 341, 21–25.
- 14 B. Liu and X. Zhao, The Synergetic Effect of V and Fe-codoping in TiO₂ Studied from the DFT+U First-principle Calculation, *Appl. Surf. Sci.*, 2017, 399, 654–662.
- 15 B. Liu, X. Wang, G. Cai, L. Wen, Y. Song and X. Zhao, Low Temperature Fabrication of V-doped TiO₂ Nanoparticles, Structure and Photocatalytic Studies, *J. Hazard. Mater.*, 2009, 169, 1112–1118.
- 16 L. Wen, B. Liu, X. Zhao, K. Nakata, T. Murakami and A. Fujishima, Synthesis, Characterization, and Photocatalysis of Fe-Doped: A Combined Experimental and Theoretical Study, *Int. J. Photoenergy*, 2012, 368750.
- 17 H. Gerischer and A. Heller, The Role of Oxygen in Photooxidation of Organic Molecules on Semiconductor Particles, *J. Phys. Chem.*, 1991, 95, 5261–5267.
- 18 W. Choi, A. Termin and M. R. Hoffmann, The Role of Metal Ion Dopants in Quantum-Sized TiO₂: Correlation between Photo reactivity and Charge Carrier Recombination Dynamics, *J. Phys. Chem.*, 1994, 98, 13669–13679.
- 19 A. Furube, T. Asahi, H. Masuhara, H. Yamashita and M. Anpo, Direct Observation of a Picosecond Charge Separation Process in Photoexcited Platinum-Loaded TiO₂ Particles by Femtosecond Diffuse Reflectance Spectroscopy, *Chem. Phys. Lett.*, 2001, 336, 424–430.
- 20 J. T. Carneiro, T. J. Savenijeb and G. Mul, Experimental Evidence for Electron Localization on Au upon Photoactivation of Au/Anatase Catalysts, *Phys. Chem. Chem. Phys.*, 2009, 11, 2708–2714.
- 21 J. L. Falconer and K. A. Magrini-Bair, Photocatalytic and Thermal Catalytic Oxidation of Acetaldehyde on Pt/TiO₂, *J. Catal.*, 1998, 179, 171–178.
- 22 J. C. Kennedy III and A. K. Datye, Photothermal Heterogeneous Oxidation of Ethanol over Pt/TiO₂, *J. Catal.*, 1998, 179, 375–389.
- 23 B. Liu, H. Wu, X. T. Zhang, I. P. Parkin and X. Zhao, New Insight into the Role of Electron Transfer to O₂ in

- Photocatalytic Oxidations of Acetone over TiO₂ and the Effect of Au Cocatalyst, *J. Phys. Chem. C*, 2019, 123, 30958–30971.
- 24 B. Dulieu, J. Bullot, J. Wéry, M. Richard and L. Brohan, Dispersive Photoconductivity in the Layered Perovskite Nd₂Ti₃O₉, *Phys. Rev. B: Condens. Matter Mater. Phys.*, 1996, 53, 10641.
- 25 Y. Muraoka, N. Takubo and Z. Hiroi, Photoinduced Conductivity in Tin Dioxide Thin Films, *J. Appl. Phys.*, 2009, 105, 103702.
- 26 V. Polliotto, S. Livraghi, A. Krukowska, M. V. Dozzi, A. Zaleska-Medynska, E. Selli and E. Giamello, Copper-Modified TiO₂ and ZrTiO₄: Cu Oxidation State Evolution during Photocatalytic Hydrogen Production, *ACS Appl. Mater. Interfaces*, 2018, 10, 27745–27756.
- 27 S. K. Poznyak, V. I. Pergushov, A. I. Kokorin, A. I. Kulak and C. W. Schlapfer, Structure and Electrochemical Properties of Species Formed as a Result of Cu(II) Ion Adsorption onto TiO₂ Nanoparticles, *J. Phys. Chem. B*, 1999, 103, 1308–1315.
- 28 A. Marimuthu, J. Zhang and S. Linic, Tuning Selectivity in Propylene Epoxidation by Plasmon Mediated Photo-Switching of Cu Oxidation State, *Science*, 2013, 339, 1590–1593.
- 29 K. Lalitha, G. Sadanandam, V. D. Kumari, M. Subrahmanyam, B. Sreedhar and N. Y. Hebalkar, Highly Stabilized and Finely Dispersed Cu₂O/TiO₂: A Promising Visible Sensitive Photocatalyst for Continuous Production of Hydrogen from Glycerol: Water Mixtures, *J. Phys. Chem. C*, 2010, 114, 22181–22189.
- 30 T. Morikawa, Y. Irokawa and T. Ohwaki, Enhanced Photocatalytic Activity of TiO_{2-x}N_x Loaded with Copper Ions under Visible Light Irradiation, *Appl. Catal., A*, 2006, 314, 123–127.
- 31 T. Morikawa, T. Ohwaki, K. Suzuki, S. Moribe and S. Tero-Kubota, Visible-Light-Induced Photocatalytic Oxidation of Carboxylic Acids and Aldehydes over N-Doped TiO₂ Loaded with Fe, Cu or Pt, *Appl. Catal., B*, 2008, 83, 56–62.
- 32 R. Katoh, A. Furube, K. Yamanaka and T. Morikawa, Charge Separation and Trapping in N-Doped TiO₂ Photocatalysts: A Time-Resolved Microwave Conductivity Study, *J. Phys. Chem. Lett.*, 2010, 1, 3261–3265.
- 33 K. Yamanaka, T. Ohwaki and T. Morikawa, Charge-Carrier Dynamics in Cu- or Fe-Loaded Nitrogen-Doped TiO₂ Powder Studied by Femtosecond Diffuse Reflectance Spectroscopy, *J. Phys. Chem. C*, 2013, 117, 16448–16456.
- 34 Quantum ESPRESSO. <http://www.quantum-espresso.org/>.
- 35 J. Wang, B. Liu and K. Nakata, Effects of Crystallinity, {001}/ {101} Ratio, and Au Decoration on the Photocatalytic Activity of Anatase TiO₂ Crystals, *Chin. J. Catal.*, 2019, 40, 403–412.
- 36 W. Zhang, Y. He, M. Zhang, Z. Yin and Q. Chen, Raman Scattering Study on Anatase TiO₂ Nanocrystals, *J. Phys. D*, 2000, 33, 912–916.
- 37 B. Liu, L. Yan and J. Wang, Liquid N₂ Quenching Induced Oxygen Defects and Surface Distortion in TiO₂ and the Effect on the Photocatalysis of Methylene Blue and Acetone, *Appl. Surf. Sci.*, 2019, 494, 266–274.
- 38 H. Irie, S. Miura, K. Kamiya and K. Hashimoto, Efficient visible light-sensitive photocatalysts: Grafting Cu(II) ions onto TiO₂ and WO₃ photocatalysts, *Chem. Phys. Lett.*, 2008, 457, 202–205.
- 39 L. Liu, F. Gao, H. Zhao and Y. Li, Tailoring Cu Valence and Oxygen Vacancy in Cu/TiO₂ Catalysts for Enhanced CO₂ Photoreduction Efficiency, *Appl. Catal., B*, 2013, 134–135, 349–358.
- 40 S. Wang, L. Pan, J.-J. Song, W. Mi, J. J. Zou, L. Wang and X. Zhang, Titanium-defected Undoped Anatase TiO₂ with p-type Conductivity, Room-temperature Ferromagnetism, and Remarkable Photocatalytic Performance., *J. Am. Chem. Soc.*, 2015, 137, 2975–2983.
- 41 B. Liu, K. Cheng, S. Nie, X. Zhao, H. Yu, J. Yu, A. Fujishima and K. Nakata, Ice–Water Quenching Induced Ti³⁺ Self-doped TiO₂ with Surface Lattice Distortion and the Increased Photocatalytic Activity, *J. Phys. Chem. C*, 2017, 121, 19836–19848.
- 42 J. Yang, B. Liu and X. Zhao, A Visible-light-active Au-Cu(I)@Na₂Ti₆O₁₃ Nanostructured Hybrid Plasmonic Photocatalytic Membrane for Acetaldehyde Elimination, *Chin. J. Catal.*, 2017, 38, 2048–2055.
- 43 X. Qiu, M. Miyauchi, K. Sunada, M. Minoshima, M. Liu, Y. Lu, D. Li, Y. Shimodaira, Y. Hosogi, Y. Kuroda and K. Hashimoto, Hybrid Cu_xO/TiO₂ Nanocomposites As Risk-Reduction Materials in Indoor Environments, *ACS Nano*, 2012, 6, 1609–1618.
- 44 M. C. Biesinger, L. W. M. Lau, A. R. Gerson and R. S. C. Smart, Resolving Surface Chemical States in XPS Analysis of First Row Transition Metals, Oxides and Hydroxides: Sc, Ti, V, Cu and Zn, *Appl. Surf. Sci.*, 2010, 257, 887–898.
- 45 A. M. Alotaibi, B. A. D. Williamson, S. Sathasivam, A. Kafizas, M. Alqahtani, C. Sotelo-Vazquez, J. Buckeridge, J. Wu, S. P. Nair, D. O. Scanlon and I. P. Parkin, Enhanced Photocatalytic and Antibacterial Ability of Cu-Doped Anatase TiO₂ Thin Films: Theory and Experiment, *ACS Appl. Mater. Interfaces*, 2020, 12, 15348–15361.
- 46 Q. Guo, Z. Ma, C. Zhou, Z. Ren and X. Yang, Single Molecule Photocatalysis on TiO₂ Surfaces, *Chem. Rev.*, 2019, 119, 11020–11041.
- 47 Y. Zhao, Y. Zhao, R. Shi, G. I. N. Waterhouse, L. Z. Wu, C.-H. Tung and T. Zhang, Tuning Oxygen Vacancies in Ultrathin TiO₂ Nanosheets to Boost Photocatalytic Nitrogen Fixation up to 700 nm, *Adv. Mater.*, 2019, 31, 1806482.
- 48 T. Morikawa, Y. Irokawa and T. Ohwaki, Enhanced Photocatalytic Activity of TiO_{2-x}N_x Loaded with Copper Ions under Visible Light Irradiation, *Appl. Catal., A*, 2008, 314, 123–127.
- 49 K. Sakaguchi, K. Shimakawa and Y. Hatanaka, Transport and Recombination of Photo-carriers under Potential Fluctuation in TiO_x Films Prepared by rf Magnetron Sputtering Method, *Phys. Status Solidi C*, 2011, 9, 2796–2799.
- 50 K. Sakaguchi, K. Shimakawa and Y. Hatanaka, Dynamic Responses of Photoconduction in TiO_x Films Prepared by Radio Frequency Magnetron Sputtering, *Jpn. J. Appl. Phys.*, 2010, 49, 091103.
- 51 K. Sakaguchi, K. Shimakawa and Y. Hatanaka, Photoconductive Characteristics of Hydro-Oxygenated Amorphous

- Titanium Oxide Films Prepared by Remote Plasma-Enhanced Chemical Vapor Deposition, *Jpn. J. Appl. Phys.*, 2006, 45, 4183–4186.
- 52 N. Golego, S. A. Studenikin and M. Cocivera, Effect of Oxygen on Transient Photoconductivity in Thin-Film $\text{Nb}_x\text{Ti}_{1-x}\text{O}_2$, *Phys. Rev. B: Condens. Matter Mater. Phys.*, 2000, 61, 8262–8269.
- 53 J. M. Herrmann, J. Disdier, M. N. Mozzanega and P. Pichat, Heterogeneous Photocatalysis: *In Situ* Photoconductivity Study of TiO_2 during Oxidation of isobutane into Acetone, *J. Catal.*, 1979, 60, 369–377.
- 54 M. I. Zaki, M. A. Hasan and L. Pasupulety, Surface Reactions of Acetone on Al_2O_3 , TiO_2 , ZrO_2 , and CeO_2 : IR Spectroscopic Assessment of Impacts of the Surface Acid-Base Properties, *Langmuir*, 2001, 17, 768–774.
- 55 A. Mattsson, M. Leideborg, K. Larsson, G. Westin and L. Österlund, Adsorption and Solar Light Decomposition of Acetone on Anatase TiO_2 and Niobium Doped TiO_2 Thin Films, *J. Phys. Chem. B*, 2006, 110, 1210–1220.
- 56 J. An, Y. Wang, J. Lu, J. Zhang, Z. Zhang, S. Xu, X. Liu, T. Zhang, M. Gocyla, M. Heggen, R. E. Dunin-Borkowski, P. Fornasiero and F. Wang, Acid-Promoter-Free Ethylene Methoxycarbonylation over Ru-Clusters/Ceria: The Catalysis of Interfacial Lewis Acid–Base Pair, *J. Am. Chem. Soc.*, 2018, 140, 4172–4181.
- 57 G. Li, N. M. Dimitrijevic, L. Chen, T. Rajh and K. A. Gray, Role of Surface/Interfacial Cu^{2+} Sites in the Photocatalytic Activity of Coupled CuO-TiO_2 Nanocomposites, *J. Phys. Chem. C*, 2008, 112, 19040–19044.
- 58 E. Iglesia, D. G. Barton, J. A. Biscardi, M. J. L. Gines and S. L. Soled, Bifunctional pathways in catalysis by solid acids and bases, *Catal. Today*, 1997, 38, 339–360.